

Fulfilling Formal Specifications ASAP by Model-free Reinforcement Learning

Mengyu Liu^{1*}, Pengyuan Lu^{2*}, Xin Chen³, Fanxin Kong¹, Oleg Sokolsky² and Insup Lee²

¹Syracuse University

²University of Pennsylvania

³University of Dayton

mliu71@syr.edu, pelu@seas.upenn.edu, xchen4@udayton.edu, fkong03@syr.edu,
{sokolsky,lee}@seas.upenn.edu

Abstract

We propose a model-free reinforcement learning solution, namely the ASAP-Phi framework, to encourage an agent to fulfill a formal specification ASAP. The framework leverages a piece-wise reward function that assigns quantitative semantic reward to traces not satisfying the specification, and a high constant reward to the remaining. Then, it trains an agent with an actor-critic-based algorithm, such as soft actor-critic (SAC), or deep deterministic policy gradient (DDPG). Moreover, we prove that ASAP-Phi produces policies that prioritize fulfilling a specification ASAP. Extensive experiments are run, including ablation studies, on state-of-the-art benchmarks. Results show that our framework succeeds in finding sufficiently fast trajectories for up to 97% test cases and defeats baselines.

1 Introduction

One significant use of model-free reinforcement learning is to train an agent to fulfill a formal specification without concrete knowledge of the environment. However, sometimes we need agents to accomplish some tasks that the state-of-the-art specification languages cannot express. For example, the agent needs to reach a goal as soon as possible (ASAP), motivated by the scenario where a real-time cyber-physical system is recovering from attacks. Unfortunately, although “accomplishing a task ASAP” is often a standard request in real-time control, how to develop a control policy based on data-driven or black box dynamics is still not well studied.

Formal languages are often used to describe control goals. For example, the reach-avoid problem on discrete and hybrid systems can be defined in linear temporal logic (LTL) [Vardi, 1996] and signal temporal logic (STL) [Raman *et al.*, 2014; Deshmukh *et al.*, 2017] respectively. Most of the existing controller synthesis approaches requires to have a formal model [Sadraddini and Belta, 2018; Donzé *et al.*, 2015; Chang *et al.*, 2019], a simulator [Ljung, 1998; Degris *et al.*, 2012; Ma *et al.*, 2021], or an identification [Qin *et al.*, 2022] of the system dynamics. Although the use of reinforcement learning (RL) in controller synthesis for black box sys-

tems has already been intensively studied [Ding *et al.*, 2011; Fu and Topcu, 2014; Li *et al.*, 2017; Li *et al.*, 2018; Hamilton *et al.*, 2022], very few work addresses the ASAP property.

Our goal is to develop real-time controllers that fulfill a formal specification ASAP for black box systems. This solution will provide a way to guide a controller synthesis procedure when formal languages are incapable of expressing certain information about the task, and in our case, the request for ASAP. In addition, once found, the solution can be applied to various scenarios. For example, it can enhance security of cyber-physical systems by solving the real-time recovery problem when the environment dynamics is unknown. The recovery problem asks an agent to find a control sequence to steer the system to a pre-defined target state within the shortest time. Existing methods leverage formal models of the system dynamics, such as ordinary differential equations (ODE), to synthesize a controller [Kong *et al.*, 2018; Zhang *et al.*, 2020; Zhang *et al.*, 2021], but to our knowledge, no work has addressed black box dynamics so far.

Our framework is called *ASAP-Phi*. It trains an agent to satisfy a given STL property with the ASAP request. Furthermore, the framework consists of: (1) constructing a particular reward function that encourages satisfying the specification ASAP, and (2) using the reward function to train a control policy on an actor-critic-based model-free RL algorithm. We prove that our ASAP-Phi framework encourages ASAP property satisfaction because any optimal policy produced must be ASAP, and design an algorithm to apply this framework to the recovery problem, to reach target sets ASAP while avoiding obstacles. The effectiveness of our approach is evaluated based on various state-of-the-art benchmarks such as OpenAI Gym [Raffin *et al.*, 2021], and the ablation studies to compare ASAP-Phi with alternative methods for deriving ASAP property. Overall, our contributions include

1. A model-free RL framework named ASAP-Phi, that takes in the information of state space, action space and a specification we want the agent to satisfy ASAP, and outputs a control policy to achieve so, without any knowledge of the environment dynamics.
2. A proof that shows any optimal policy produced by ASAP-Phi indeed achieves a property ASAP.
3. Experiments demonstrate that ASAP-Phi has up to 97% high rate to succeed in tasks that requires ASAP behav-

*These authors contributed equally to this work

iors and beats baseline methods, as well as ablation studies that show its advantages over alternative approaches.

2 Preliminaries

2.1 Notations

In the paper, we use \mathcal{S} to denote the *state space* of a system. A *trajectory* (or trace) is a finite sequence of states $\bar{s} = s_1, \dots, s_k$ such that $s_i \in \mathcal{S}$ for all $i = 1, \dots, k$. We only consider discrete trajectories of the system and we sometimes use s_t to denote the system state at the time t . The notation \mathcal{A} stands for the set of *actions* that can be applied to the system. The rest of the notations will be introduced along the paper upon their appearances.

2.2 Actor-critic RL

Actor-critic RL is a class of model-free RL algorithms that maintains and updates two models, which represents the learned policy (actor) π and the estimated value function (critic) v , respectively. The training is to search for an optimal v^* that estimates the expected value, and an optimal π^* that maximizes the estimated value. Formally,

$$\begin{aligned} v_\pi^*(s_t) &= \mathbb{E}_\pi[r(s_t) + \gamma v^*(s_{t+1}) | s_t] \\ \pi^*(s_t) &= \arg \max_\pi v_\pi^*(s_t). \end{aligned} \quad (1)$$

where r is the reward function, s_t, s_{t+1} are the current and next system state respectively. \mathbb{E}_π denotes the expectation under the policy π , and $0 < \gamma < 1$ is the discount factor. Finding the solutions to Equation (1) is the goal of actor-critic RL [Peters *et al.*, 2005]. Here, the optimal v^* is a solution to the recursive Bellman equation that depends on the policy selected, and the optimal π^* aims to maximize the expectation.

There are various methods to implement an actor-critic RL. For example, soft actor-critic (SAC) leverages entropy of distributions to regularize the value estimation [Haarnoja *et al.*, 2018]. Deep deterministic policy gradient (DDPG) treats policies as deterministic and uses delayed copies of actor and critic models to improve robustness against training data variance [Silver *et al.*, 2014]. We can find well developed methods from the Stable Baselines module [Raffin *et al.*, 2021].

2.3 Formal Specifications and STL

In the area of formal methods, formal specifications are unambiguous descriptions of the tasks that we want agents to accomplish. They can be expressed in multiple formal languages, for example, linear temporal logic (LTL [Vardi, 1996] and signal temporal logic (STL) [Raman *et al.*, 2014; Deshmukh *et al.*, 2017]. In this paper, we focus on STL. An STL formula can be defined using the following syntax:

$$\varphi ::= \top \mid f(\bar{s}) < 0 \mid \neg\varphi \mid \varphi_1 \wedge \varphi_2 \mid \varphi_1 U_{[t_1, t_2]} \varphi_2 \quad (2)$$

such that \top is tautology, and f is a function that maps a trajectory (or equivalently, a signal, in the context of STL) \bar{s} to a real number. U is the until operator, e.g., $\varphi_1 U_{[t_1, t_2]} \varphi_2$ indicates that φ_2 must hold at some time $t \in [t_1, t_2]$ and φ_1 must always hold before that. The time interval $[t_1, t_2]$ is interpreted as $\{t_1, t_1 + 1, \dots, t_2\}$. Based on this grammatical

structure, STL has guided control synthesis in the field of optimal control [Sadraddini and Belta, 2018; Donz  *et al.*, 2015; Raman *et al.*, 2014]. However, we must admit there is a certain lack of expressiveness of STL and other formal languages, such as they cannot express some common requirements to humans like "as soon as possible".

2.4 Specification-guided RL

Existing work in RL tried multiple ways to leverage formal specification to guide agent training. Specifically, there are two major approaches in the current state-of-the-art. First, some construct a product Markov decision process (MDP) to combine the underlying MDP and the specification, which is transformed into a finite state machine [Fu and Topcu, 2014; Ding *et al.*, 2011]. Alternatively, less guaranteed but more flexible approach is to construct a reward function based on the formal specification. For example, quantitative semantics is a real-valued measure ρ on how much a signal \bar{s} satisfies an STL property φ at time t [Hamilton *et al.*, 2022]. We restate its definition in our notations as follows.

$$\begin{aligned} \rho(\bar{s}, t, (f(\bar{s}) < d)) &= d - f(s_t) \\ \rho(\bar{s}, t, \neg\varphi) &= -\rho(\bar{s}, \varphi, t) \\ \rho(\bar{s}, t, \varphi_1 \wedge \varphi_2) &= \min(\rho(\bar{s}, t, \varphi_1), \rho(\bar{s}, t, \varphi_2)) \\ \rho(\bar{s}, t, \varphi_1 \vee \varphi_2) &= \max(\rho(\bar{s}, t, \varphi_1), \rho(\bar{s}, t, \varphi_2)) \\ \rho(\bar{s}, t, F_{[t_1, t_2]} \varphi) &= \max_{t' \in [t'+t_1, t'+t_2]} \rho(\bar{s}, t', \varphi) \\ \rho(\bar{s}, t, G_{[t_1, t_2]} \varphi) &= \min_{t' \in [t'+t_1, t'+t_2]} \rho(\bar{s}, t', \varphi) \\ \rho(\bar{s}, t, \varphi_1 U_{[t_1, t_2]} \varphi_2) &= \max_{t' \in [t'+t_1, t'+t_2]} \left(\min(\rho(\bar{s}, t', \varphi_2), \min_{t'' \in [t, t']} \rho(\bar{s}, t'', \varphi_1)) \right) \end{aligned} \quad (3)$$

Here, for convenience, we introduce the finally (F) and globally (G) operators which can be defined using U , i.e., $F_I \varphi = \top U_I \varphi$ and $G_I \varphi = \neg(\top U_I \neg\varphi)$ where I is a time interval. By the construction of Equation (3), we are able to evaluate a real-valued degree of property satisfaction of the current state so far. Therefore, people have been using this score in reward functions via various ways to guide RL [Hamilton *et al.*, 2022; Li *et al.*, 2017; Li *et al.*, 2018]. However, because these metrics are derived from STL satisfaction, they still lack the expressiveness when describing certain tasks in the same way of STL. As a response, researchers have proposed sophisticated reward shaping techniques so that the score can encourage and discourage agent behaviors more accurately [Berducci *et al.*, 2021]. However, to our knowledge, little has been done on expressing ASAP, which is vital to the CPS recovery problem introduced in the next subsection.

2.5 Real-time Cyber-physical System Recovery

Cyber-physical systems (CPS) are (usually real-time) software-controlled agents that interacts with the physical world. For instance, autonomous vehicles, robots, smart power grids and medical devices are all CPS. Recently, one problem, namely CPS recovery, have been widely discussed by researchers. Specifically, when a CPS finds itself in an

undesirable state, how to guide it back to a predefined safe target set of states?

Researchers have discussed some harder versions of this problem. For example, some discuss the guidance when an agent’s sensors are under attack so that the observed states are unreliable [Kong *et al.*, 2018; Zhang *et al.*, 2020; Zhang *et al.*, 2021]. However, most of the works assume a known environment dynamics so that the recovery controller can be synthesized by optimal control algorithms. We focus on a more severe case, where the dynamics is an unknown black-box, but we are able to sample data points from it for agent training purposes. Overall, our work explore how to patch up insufficient expressiveness of formal specifications in this real world-motivated scenario.

3 Problem Formulation

Our problem is motivated by the real-time CPS recovery problem defined in Section 2. That is, in certain scenarios we want an agent, which is not currently satisfying some property, such as ASAP. For instance, in the recovery problem, we want the agent to reach a pre-defined target state set ASAP.

Specifically, we would like to build a framework that inputs a state space \mathcal{S} , an action space \mathcal{A} , and a specified STL property φ . The framework outputs a control policy $\pi(a_t|s_t)$, i.e., a probability distribution of actions given a state, such that the satisfaction of φ is ASAP.

Given a trace $\bar{s} = s_0s_1\dots s_k$ for some $k \geq 0$, we use $(\bar{s}, t) \models \varphi$ where $0 \leq t \leq k$ to denote that the state s_t satisfies the property φ . Then, we define a function $t_\varphi(\cdot)$ that evaluates the first time step that a signal satisfies a property as follows.

$$t_\varphi(\bar{s}) = \begin{cases} \infty, & \nexists t \in \{0, \dots, k\}, (\bar{s}, t) \models \varphi \\ \arg \min_{t \in \{0, \dots, k\}} ((\bar{s}, t) \models \varphi), & \text{otherwise.} \end{cases} \quad (4)$$

Intuitively, $t_\varphi(s) = \infty$ if there is no time step that s satisfies φ . Otherwise, it is the first time step of satisfaction.

We say that a policy π^* is ASAP if it has a higher probability to sample a trace that satisfies the given property within a shorter time, under an unknown probabilistic underlying system model, i.e., a state transition distribution $p(s_{t+1}|s_t, a_t)$.

Definition 1 (ASAP Policies). *On a state space \mathcal{S} , an action space \mathcal{A} , and an underlying system model p , we say a policy π^* is ASAP iff for two arbitrary traces \bar{s} and \bar{s}' that both start at an arbitrary initial state s_0 ,*

$$t_\varphi(\bar{s}) < t_\varphi(\bar{s}') \implies \Pr_{p, \pi^*}(\bar{s}'|s_0) < \Pr_{p, \pi^*}(\bar{s}|s_0) \quad (5)$$

We propose an approach to find such an optimal policy based on the following assumptions.

Assumption 1: *A system is always maintainable once property is reached.* When a system satisfies the given property φ , then it has the highest probability to be maintained to keep satisfying the property using some control inputs. Notice that this assumption is reasonable, since a target set in the recovery problem is often a neighborhood of a stable equilibrium [Abad *et al.*, 2016; Abdi *et al.*, 2018]. Once inside this neighborhood, the agent’s behavior will be stabilized and we can assume a constant expected cumulative reward in the future, i.e. for any policy π , on any trajectory \bar{s}' that continues

on some \bar{s} ,

$$(|\bar{s}| = t) \wedge ((\bar{s}, t) \models \varphi) \implies \mathbb{E}_\pi \left[\sum_{t'=t+1}^{\infty} \gamma^{t'} r(s'_{t'}) | \bar{s}'_{0:t} = \bar{s} \right] = M \quad (6)$$

where M is a constant and $\bar{s}'_{0:t}$ denotes the sub-trace from time step 0 to t of \bar{s}' . In other words, if \bar{s} satisfies the property in its last time step, then every trace that extends from it has a fixed expected cumulative reward afterwards due to stability.

Assumption 2: *The length and the semantics score of a trace are always bounded.* Firstly, our RL framework only considers the system traces which are length-bounded. We denote the bounds k_{min} and k_{max} . Secondly, we assume that all system traces have bounded quantitative semantics scores. We denote the bounds ρ_{min} and ρ_{max} .

Assumption 3: *The blackbox (unknown) system performs as a Markov Decision Process.* Precisely, any action from the system is performed only based on the current state. Therefore, all traces generated by the system has a probability which is independent from the others.

We seek to solve the following two problems:

Problem 1: Given a blackbox system along with its state space \mathcal{S} and action space \mathcal{A} . How can we learn an ASAP policy π^* regarding to an STL property φ ?

Problem 2: How can we leverage the ASAP policy obtained by solving Problem 1 and use it to solve the system recovery problem?

4 The ASAP-Phi Framework

4.1 The Workflow

For Problem 1, we propose the following framework, namely ASAP-Phi, which consists of generating a piece-wise reward function and training on actor-critic-based model-free RL algorithms, while the training requires sampling from the underlying transition distribution $p(s_{t+1}|s_t, a_t)$.

First, we design a deterministic piece-wise reward function r_{asap} as follows.

$$r_{asap}(\bar{s}, t, \varphi) = \begin{cases} \rho(\bar{s}, t, \varphi), & \text{if } (\bar{s}, t) \not\models \varphi \\ r_{sat} \gg \rho_{max}, & \text{otherwise} \end{cases} \quad (7)$$

Equation (7) defines a reward function that evaluates on a trace \bar{s} w.r.t. an STL property φ and a maximum time index t . It splits the reward into two cases: If the signal until t does not satisfy the given property, we use the quantitative semantics score ρ , defined in Section 2.4, to evaluate the degree of property satisfaction; otherwise, we pick a large constant r_{sat} that is greater than all possible rewards in the previous case. Notice that, to compute this reward, we need to keep the whole trace \bar{s} to check the property satisfaction. This large constant will be discussed in the next subsection.

Usually, the quantitative semantics produce sparse reward since it only compute the degree of the robustness at the end of the episode which is also known as sparse reward [Hamilton *et al.*, 2022]. And the return is the degree of the robustness for the whole episode. Alternatively, there is also a dense reward option for the quantitative semantics where the degree of the robustness is computed at each time step. The return of the dense reward represents the degree of robustness for the

subtrajectory from the start to the current time step. In this paper, we proposed a variation of the dense reward: Finite dense reward which evaluates the degree of the robustness of the trajectory contains the most recent d time steps, d is a hyperparameter.

We present our RL framework in Algorithm 1. The main loop iteratively generates a random trace whose length is in the specific range. It progressively updates a policy (actor) model π_θ parameterized by θ and a value (critic) model v_w parameterized by w by calling an external actor-critic-based algorithm, denoted by AC , that can be soft actor-critic (SAC) [Haarnoja *et al.*, 2018] or deep deterministic policy gradient (DDPG) [Silver *et al.*, 2014].

Algorithm 1 ASAP-Phi (on-policy version)

Input: Reward function r_{asap} , state space \mathcal{S} , action space \mathcal{A} , STL property φ , actor-critic training algorithm AC , system model p that is unknown but allows sampling, number of training samples m , lower and upper bound of episode length k_{\min} and k_{\max}

Output: Control policy π_θ

- 1: Initialize policy model π_θ and value model v_w
 - 2: $m_{train} \leftarrow 0$
 - 3: **while** $m_{train} < m$ **do**
 - 4: $k \leftarrow$ uniformly sample from $[k_{\min}, k_{\max}]$
 - 5: $s_0 \leftarrow$ uniformly sample from \mathcal{S}
 - 6: Cached signal $\bar{s} \leftarrow [s_0]$
 - 7: **for** $t = 0, \dots, k$ **do**
 - 8: $r \leftarrow r_{asap}(\bar{s}, t, \varphi)$
 - 9: $a_t \leftarrow$ sample from $\pi_\theta(\cdot | s_t)$
 - 10: $s_{t+1} \leftarrow$ sample from $p(\cdot | s_t, a_t)$
 - 11: Append s_{t+1} to \bar{s}
 - 12: $\pi_\theta, v_w \leftarrow AC(s_t, a_t, s_{t+1}, r)$
 - 13: $m_{train} \leftarrow m_{train} + 1$
 - 14: **end for**
 - 15: **end while**
-

Algorithm 1 trains the policy and value models on m data points, which combines to multiple trace episodes of lengths between k_{\min} and k_{\max} . Specifically, the outer loop from line 3 to 14 represents the entire procedure on all episodes, and the inner loop from line 7 to 13 is one episode. The training is at line 11, where the actor-critic algorithm updates the two models using \bar{s}_t , a_t and \bar{s}_{t+1} , on our designed reward function r_{asap} . Notice that this version of algorithm is on-policy. That is, there is one model update per arrival of new data point. We can also leverage off-policy training by moving the model update at the end of every episode.

4.2 Proof of Correctness

In this subsection, we prove the correctness of ASAP-Phi, i.e., if ASAP-Phi returns an optimal policy, then it is also ASAP.

Theorem 2 (ASAP-Phi Correctness). *The optimal policy learned from ASAP-Phi framework is an ASAP policy.*

Proof. We prove the theorem by contradiction. Assume that there is an optimal policy π^* learned by ASAP-Phi, and it is

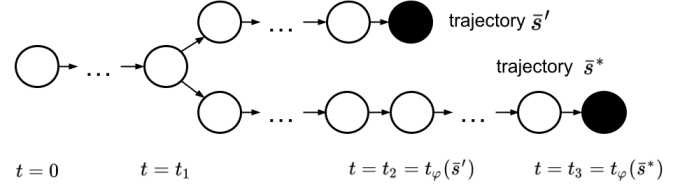


Figure 1: The two existing trajectories under the assumed π^* . An empty circle represents the trajectory so far does not satisfy φ , while a filled circle means satisfy.

not ASAP. We seek to prove that π^* is also not optimal that contradicts our assumption.

Given that π^* is optimal but not ASAP, then there exists two traces \bar{s}^* and \bar{s}' both of which start from an initial state s_0 and reach a target state as their last states. We also have that $\Pr_{p, \pi^*}(\bar{s}' | s_0) < \Pr_{p, \pi^*}(\bar{s}^* | s_0)$ and $|\bar{s}'| < |\bar{s}^*|$ by assumption, i.e., \bar{s}^* is longer than \bar{s}' but the former one has a higher probability to be performed than the later one using π^* . We illustrate these two traces in Figure 1. Here, t_1 is the last time that the two traces are exactly identical since beginning, t_2 is the time for \bar{s}' to satisfy φ for the first time, and t_3 is for \bar{s}^* .

By Assumption 1, a trace can be maintained in the target set when it reaches there. We therefore construct a trajectory by padding satisfactory states after \bar{s}' until time t_3 . We denote this trajectory as \bar{s}'' . Then we have that, $\Pr_{p, \pi^*}(\bar{s}'' | s_0) \leq \Pr_{p, \pi^*}(\bar{s}' | s_0) < \Pr_{p, \pi^*}(\bar{s}^* | s_0)$, since \bar{s}'' is an extension of \bar{s}' .

Since the v^* is also optimal, it is a solution to the Bellman equation (1):

$$v_{\pi^*}^*(s_0) = \mathbb{E}_{\pi^*} \left[\sum_{t=0}^{\infty} \gamma^t r_{asap}(\bar{s}, t, \varphi) | s_0 \right] = \mathbb{E}_{\pi^*} \left[\sum_{t=0}^{t_3} \gamma^t r_{asap}(\bar{s}, t, \varphi) | s_0 \right] + \underbrace{\mathbb{E}_{\pi^*} \left[\sum_{t=t_3+1}^{\infty} \gamma^t r_{asap}(\bar{s}, t, \varphi) | s_0 \right]}_{\text{denote this term } D_{\pi^*}} \quad (8)$$

and therefore

$$\begin{aligned} v_{\pi^*}^*(s_0) &= \mathbb{E}_{\pi^*} \left[\sum_{t=0}^{t_3} \gamma^t r_{asap}(\bar{s}, t, \varphi) | s_0 \right] + D_{\pi^*} \\ &= p_1 \underbrace{\sum_{t=0}^{t_3} \gamma^t r_{asap}(\bar{s}^*, t, \varphi)}_{\text{denote this term } A} + p_2 \underbrace{\sum_{t=0}^{t_3} \gamma^t r_{asap}(\bar{s}'', t, \varphi)}_{\text{denote this term } B} \\ &\quad + \underbrace{\mathbb{E}_{\pi^*} \left[\sum_{t=0}^{t_3} \gamma^t r_{asap}(\bar{s}, t, \varphi) | s_0, \bar{s} \neq \bar{s}^* \wedge \bar{s} \neq \bar{s}'' \wedge |\bar{s}| = t_3 \right]}_{\text{denote this term } C_{\pi^*}} + D_{\pi^*} \\ &= p_1 A + p_2 B + C_{\pi^*} + D_{\pi^*} \quad (9) \end{aligned}$$

where $p_1 = \Pr_{p, \pi^*}(\bar{s}^* | s_0)$, $p_2 = \Pr_{p, \pi^*}(\bar{s}'' | s_0)$. That is, the probabilities to take traces \bar{s}^* and \bar{s}'' , respectively. The term C_{π^*} denotes the value to be obtained by taking any other trace of length t_3 starting from s_0 under policy π^* .

We now construct an alternative policy π' , by swapping the probabilities p_1 and p_2 on the two traces. We are able to do so because of Assumption 3, that all trajectories are independent from each other due to the Markovian state transitions. Then we have the following new value estimation:

$$v_{\pi'}^*(s_0) = p_2A + p_1B + C_{\pi'} + D_{\pi'} \quad (10)$$

Since all the traces of the length t_3 other than \bar{s}^* and \bar{s}'' have the same probabilities in π^* and π' , thus $C_{\pi'} = C_{\pi^*}$. Moreover, by Assumption 1, since both \bar{s}'' and \bar{s}^* enters the stable neighborhood at time t_3 , we can leverage Equation (6) and get

$$\begin{aligned} D_{\pi'} &= \mathbb{E}_{\pi} \left[\sum_{t=t_3+1}^{\infty} \gamma^t r_{\text{asap}}(\bar{s}, t, \varphi) | s_0 \right] \\ &= \mathbb{E}_{\pi} \left[\sum_{t=t_3+1}^{\infty} \gamma^t r_{\text{asap}}(\bar{s}, t, \varphi) | s_0, \bar{s}_{0:t_3} = \bar{s}^* \right] \\ &\quad + \mathbb{E}_{\pi} \left[\sum_{t=t_3+1}^{\infty} \gamma^t r_{\text{asap}}(\bar{s}, t, \varphi) | s_0, \bar{s}_{0:t_3} = \bar{s}'' \right] \\ &\quad + \mathbb{E}_{\pi} \left[\sum_{t=t_3+1}^{\infty} \gamma^t r_{\text{asap}}(\bar{s}, t, \varphi) | s_0, \bar{s} \neq \bar{s}^* \wedge \bar{s} \neq \bar{s}'' \right] \\ &= 2M + \mathbb{E}_{\pi} \left[\sum_{t=t_3+1}^{\infty} \gamma^t r_{\text{asap}}(\bar{s}, t, \varphi) | s_0, \bar{s}_{0:t_3} \neq \bar{s}^* \wedge \bar{s}_{0:t_3} \neq \bar{s}'' \right] \\ &= D_{\pi^*} \end{aligned} \quad (11)$$

where $\bar{s}_{0:t_3}$ denotes the sub-trace from time step 0 to t_3 of a trace \bar{s} . Therefore, we also have that $D_{\pi'} = D_{\pi^*}$. Then we only need to compare $p_1A + p_2B$ and $p_2A + p_1B$.

By the definition of r_{asap} in (7), we have that

$$\begin{aligned} A &= \underbrace{\sum_{t=0}^{t_1} \gamma^t \rho(\bar{s}^*, t, \varphi)}_{A_1} + \underbrace{\sum_{t=t_1+1}^{t_2} \gamma^t \rho(\bar{s}^*, t, \varphi)}_{A_2} + \underbrace{\sum_{t=t_2+1}^{t_3} \gamma^t \rho(\bar{s}^*, t, \varphi)}_{A_3} \\ B &= \underbrace{\sum_{t=0}^{t_1} \gamma^t \rho(\bar{s}'', t, \varphi)}_{B_1} + \underbrace{\sum_{t=t_1+1}^{t_2} \gamma^t \rho(\bar{s}'', t, \varphi)}_{B_2} + \underbrace{\sum_{t=t_2+1}^{t_3} \gamma^t r_{\text{sat}}}_{B_3} \end{aligned} \quad (12)$$

Since the two traces \bar{s}^* and \bar{s}'' are identical from $t = 1$ to $t = t_1$, we have that $A_1 = B_1$. Also, since $r_{\text{sat}} > \rho_{\max}$, we have that $A_3 < B_3$. For the last pair A_2 and B_2 , we have that

$$\begin{aligned} A_2 - B_2 &= \sum_{t=t_1+1}^{t_2} \gamma_t (\rho(\bar{s}^*, t, \varphi) - \rho(\bar{s}'', t, \varphi)) \\ &\leq \sum_{t=t_1+1}^{t_2} \gamma_t (\rho_{\max} - \rho_{\min}) \leq (\rho_{\max} - \rho_{\min}) \sum_{t=0}^{k_{\max}} \gamma_t \\ &\leq (\rho_{\max} - \rho_{\min}) k_{\max} \end{aligned} \quad (13)$$

Therefore, if we set $r_{\text{sat}} > \rho_{\max} + (\rho_{\max} - \rho_{\min}) k_{\max}$, we can guarantee that $A_2 - B_2 < B_3 - A_3$. Hence, we have $A < B$. Recall that $p_1 > p_2$, so $p_2A + p_1B > p_1A + p_2B$, i.e., $v_{\pi'}^*(s_0) > v_{\pi^*}^*(s_0)$. Therefore, π' is better than π^* , or π^* is not an optimal policy. \square

4.3 ASAP-Phi in Recovery Problem

ASAP-Phi is a general solution that can drive a system from a deviated state (that does not satisfy a property) to a target state (that satisfies it). While not explicitly dedicated to the security aspect, our solution positively enhances the resilience to faults and attacks. For specific fault or attack scenarios, certain adaptations to our solution may be needed. As an use case, we propose the following use of ASAP-Phi to solve the CPS recovery problem and answer Problem 2.

In the recovery problem, we have a target set of states $\mathcal{S}_T \subset \mathcal{S}$ that we want an agent to reach it ASAP. Optionally, there may exist certain states $\mathcal{S}_O \subset \mathcal{S}$ that represents obstacles or danger zones that we want to avoid, $\mathcal{S}_T \cap \mathcal{S}_O = \emptyset$. The target set and obstacle set are assumed to be bounded, so we can check whether a state s_t is contained inside efficiently. Therefore, we specify these two requirements using STL properties:

$$\varphi_T = s_t \in \mathcal{S}_T, \quad \varphi_O = s_t \notin \mathcal{S}_O \quad (14)$$

In other words, we want to learn a policy that satisfies φ_T ASAP while always satisfying φ_O . Therefore, we need to measure the degree of robustness for φ_T as reward for training. Additionally, we need to have reward shaping to make sure the optimal policy can satisfy φ_O . We leverage the ASAP-Phi training in Algorithm 1 to do so, by taking regular policy and value function updates on φ_T , and early stop once a sampled trace violates φ_O . For convenience, we wrap up the initialization of ASAP-Phi for each episode as a canonical subroutine *ASAP_phi_ep_init()* (line 4-5 of Algorithm 1), and each update step in the inner loop as *ASAL_phi_step()* (line 8-12 of Algorithm 1), with the reward function designed based on a property φ . The solution is stated in Algorithm 2

Algorithm 2 ASAP-Phi for Recovery

Input: Properties φ_T , φ_O and everything else required by Algorithm 1

Output: Recovery control policy π_{θ}

- 1: Initialize policy model π_{θ} and value model v_w
 - 2: $m_{\text{train}} \leftarrow 0$
 - 3: **while** $m_{\text{train}} < m$ **do**
 - 4: *ASAP_phi_ep_init()*
 - 5: **for** $t = 0, \dots, |\bar{s}| - 1$ **do**
 - 6: **if** $(\bar{s}, t) \not\models \varphi_O$ **then**
 - 7: break
 - 8: **end if**
 - 9: $\pi_{\theta}, v_w \leftarrow \text{ASAL_phi_step}(\varphi_T)$
 - 10: $m_{\text{train}} \leftarrow m_{\text{train}} + 1$
 - 11: **end for**
 - 12: **end while**
-

Notice that the key idea is to search for an optimal policy that is ASAP to satisfy φ_T and early stop on violation of φ_O . The reason to do so is to prevent the trajectory from getting the high reward r_{sat} if it enters an obstacle state, such that the agent will learn to take alternative paths to reach a target state ASAP. We demonstrate the effectiveness of this approach in the experiment section.

5 Experimental Evaluations

5.1 Setup

We set up groups of experiments on recovery problems for evaluation. The experiments are implemented on four benchmarks: DC Motor Position, Bicycle, Attitude Control and Mujoco Swimmer. DC Motor Position is a classical system from control community and CPS community, with a goal to control a motor’s rotation angle by direct current [Zhang *et al.*, 2020]. Bicycle benchmark simulates the dynamics of a bicycle with two control inputs: steering angle and acceleration [Kong *et al.*, 2015], with a goal to ride the bicycle at different speeds and directions. Attitude Control benchmark is from the artificial intelligence category of Workshop on Applied Verification for Continuous and Hybrid Systems (ARCH-COMP’22) [Lopez *et al.*, 2022], with a goal to control the rigid body to avoid unsafe area. Finally, the Mujoco Swimmer benchmark is one of the well-known Mujoco environments for reinforcement learning [Brockman *et al.*, 2016; Todorov *et al.*, 2012], aiming to control the two-joints system and move to the right as fast as possible. More detailed descriptions of the benchmarks can be found in Appendix. Although some of the benchmarks have formal models such as ODEs, our approach only uses their simulators as black boxes.

We select classical actor-critic based training algorithms including SAC, DDPG, A2C, TD3 and PPO. To avoid the performance decay from the implementation of these algorithms, we use the implementation from stable baselines 3 which developed and maintained by OpenAI [Raffin *et al.*, 2021]. For each benchmark, there is a given target set and a unsafe set. These two sets are defined as balls for simplification. We train agents to find policies that make the system reach the target set ASAP without touching the unsafe set.

Despite our proof in Section 4.2, it is generally hard to find an optimal policy by training, so we seek sub-optimal policies, i.e., recovery within a selected maximum time tolerance, which is similar to the evaluation metrics for recovery tasks used in previous work [Zhang *et al.*, 2020; Zhang *et al.*, 2021; Kong *et al.*, 2018]. We consider two types of recovery tasks: *Reach* and *Reach&Avoid*. For *Reach* tasks, unsafe obstacle states are absent. For *Reach&Avoid* tasks, the system should avoid a pre-defined obstacle set, as described in Section 4.3. We test the trained agents on 1000 random initial points and count how many traces can reach the target set within the maximum time tolerance. A trace will be terminated if it touches the obstacle and considered a failure for *Reach&Avoid* tasks. We calculate the success rate of the traces generated by policies to evaluate their performance.

We compare the performance between ASAP-Phi and other baseline rewards as main results. Additionally, we do ablation studies on ASAP-Phi to show ASAP-Phi’s insensitivity to training algorithms. For more details about experiment, please see appendix.

5.2 Main Results

We choose two reward function baselines to compare with ASAP-Phi. One is quantitative semantics reintroduced in section 2.4, which represents the degree of satisfaction of a given

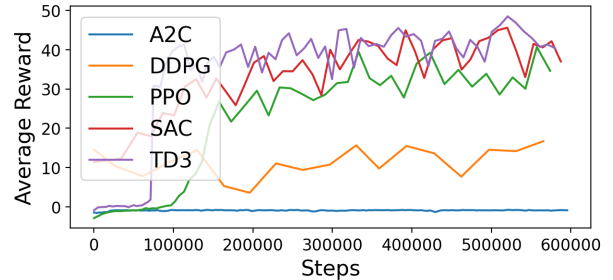


Figure 2: Training history of Swimmer on *Reach&Avoid* task

STL specification [Hamilton *et al.*, 2022]. We denote this reward as ρ -reward. Another reward function baseline is heuristic distance-based reward function which is widely applied in existed works [Burchfiel *et al.*, 2016; Trott *et al.*, 2019; Li *et al.*, 2017], and we restate it as follows to avoid abuse of notations.

$$r_d = -\lambda_T d_T + \lambda_O d_O + r_{base} \quad (15)$$

where d_T and d_O are the distances to the target set \mathcal{S}_T and the unsafe obstacle set \mathcal{S}_O , respectively, and λ_T , λ_O and r_{base} are hyperparameters.

We use SAC to train the agents for the main results. From Table 1, there are three main observations:

1. ASAP-Phi outperform baselines in most cases. We can see ASAP-Phi have more than 50% success rate for every cases and defeats the two baselines for most trials. In only a few cases, for example, the *Reach&Avoid* task on bicycle benchmark, the ρ -reward performs slightly better than ASAP-Phi. This small difference can be from due to the noise in training since there is no guarantee that the optimal policy is found.
2. ASAP-Phi’s performance is much more stable than the other two baselines. For example, the d -reward baseline performs much worse than others on most tasks but slightly outperform others on *Reach&Avoid* task for DC Motor Position if the maximum time tolerance is 15 time steps. This instability does not happen to ASAP-Phi.
3. Sometimes an agent can achieve better performance on *Reach&Avoid* tasks than *Reach* tasks. Intuitively, *Reach&Avoid* tasks are harder than *Reach* tasks. However, it is hard to find optimal policies through training, so there can be performance difference between tasks.

Since ASAP-Phi outperforms the baselines for the majority of cases, we state that ASAP-Phi is effective to achieve a given specification ASAP in practice.

5.3 Ablation Studies

We conduct ablation studies on (1) different actor-critic algorithms and (2) different ways to encourage ASAP other than the current reward functions. Here, we present the results of the former in Table 2, with two main observations.

1. ASAP-Phi is not designed for a particular training algorithm. In other words, Table 2 have shown the insensitivity to the training algorithms. On contrary, ASAP-Phi is

Max Time Tolerance*	Method	DC Motor Position		Bicycle		Attitude Control		Swimmer	
		<i>R</i>	<i>R&A</i>	<i>R</i>	<i>R&A</i>	<i>R</i>	<i>R&A</i>	<i>R</i>	<i>R&A</i>
30	ASAP-phi	97.4%	97.8%	92.8%	91.0%	93.9%	92.0%	62.6%	64.1%
	ρ -reward	83.5%	82.1%	80.6%	86.4%	75.1%	73.6%	58.4%	57.2%
	d -reward	35.5%	95.3%	78.4%	27.6%	21.1%	12.7%	42.5%	6.5%
25	ASAP-phi	95.2%	95.3%	88.1%	89.2%	86.5%	85.3%	57.4%	59.3%
	ρ -reward	77.3%	79.8%	80.6%	86.1%	72.4%	70.9%	51.5%	50.8%
	d -reward	32.2%	95.1%	76.2%	27.0%	18.0%	11.9%	39.4%	6.1%
15	ASAP-phi	89.0%	84.9%	74.4%	65.1%	55.7%	52.0%	52.0%	53.0%
	ρ -reward	59.2%	79.4%	72.6%	65.5%	52.2%	51.9%	47.4%	46.0%
	d -reward	29.2%	87.0%	65.4%	25.3%	15.6%	10.7%	34.1%	4.8%

Table 1: Agent performance measured by successful recovery rate. Here, *R* and *R&A* denote *Reach* and *Reach&Avoid* tasks, respectively. *: For swimmer, the maximum time tolerance are 50, 40, 30 time steps instead of 30, 25, 15.

	DC Motor Position		Bicycle		Attitude Control		Swimmer	
	<i>Reach</i>	<i>Reach&Avoid</i>	<i>Reach</i>	<i>Reach&Avoid</i>	<i>Reach</i>	<i>Reach&Avoid</i>	<i>Reach</i>	<i>Reach&Avoid</i>
SAC	97.4%	97.8%	83.0%	78.8%	75.6%	74.1%	62.6%	64.1%
DDPG	99.6%	95.7%	75.8%	78.2%	62.7%	61.6%	11.5%	11.8%
A2C	56.8%	39.3%	37.8%	22.8%	15.2%	14.3%	0.6%	0.4%
TD3	99.0%	96.3%	76.8%	81.4%	78.4%	77.6%	62.8%	54.1%
PPO	37.8%	39.6%	79.9%	80.2%	65.0%	64.8%	15.2%	13.1%

Table 2: Success rate of traces produced by policies trained by different algorithms, the maximum time tolerance is set to 30 time steps for DC Motor Position, 20 time steps for Bicycle and Attitude Control, the maximum time tolerance is set to 50 for Swimmer benchmark.

compatible with various actor-critic-based methods. For example, SAC and TD3 perform the best among the five algorithms tested. DDPG also have good performance on several tasks as Fig. 2 shows.

- The performance of PPO and A2C are not stable. For example, PPO perform poorly on the Swimmer benchmark and A2C perform worse than other algorithms in general for the two tasks.

In the second ablation study on different ways of encouraging ASAP, we found that our current reward performs the best. Please refer to Appendix for the results and other details.

6 Discussion

Advantages of ASAP-Phi. From the analysis in Section 4.2 we prove that ASAP-Phi is seeking an optimal policy that maximizes the probability to choose a trace to satisfy a given formal specification ASAP, using only sampled training data but no system dynamics knowledge. To our knowledge, such a framework is yet to be proposed by existing work, despite its necessity in various applied scenarios such as CPS recovery. Moreover, although it is commonly hard to achieve this theoretical optimal policy in implementation, our experiments in Section 5 show that ASAP-Phi achieve high success

rate to recover an agent within deadline, up to 97% and defeating state-of-the-art baselines in general.

Limitations of ASAP-Phi. However, there indeed exist certain limitations. First, ASAP-Phi is based on model-free RL, which means it naturally inherits the disadvantages of this class of learning algorithms. For example, it requires collection of sufficient training data and tuning of learning hyperparameters. Fortunately, this is partially resolved by researchers designing stable actor-critic backbones [Raffin *et al.*, 2021]. Second, although we have explored various ways to encourage ASAP, the reward function 7 may not necessarily be the best approach. Therefore, how to encourage the learning of an ASAP policy remains an open problem. Finally, the framework makes several assumptions. Although Assumptions 1-3 in Section 3 are reasonable in the current context, so far it is unknown how to lift these assumptions while still obtaining an ASAP policy. The system dynamics, though a black box, is assumed to be static and allowing an arbitrary amount of data sampling - yet another assumption to be lifted. We believe these can be topics studied in future works.

7 Conclusion

Motivated by the real-time CPS recovery problem under unknown system dynamics, we propose ASAP-Phi, a model-

free RL framework that encourages fulfilling an STL formal specification ASAP. We prove that the optimal policy learned by ASAP-Phi is indeed ASAP and apply it back to the motivating case study of recovery. Experiments show that control policies trained by ASAP-Phi constantly achieve high success rate of recovery within the maximum time tolerance and generally defeat baselines on state-of-the-art benchmarks.

References

- [Abad *et al.*, 2016] Fardin Abdi Taghi Abad, Renato Mancuso, Stanley Bak, Or Dantsker, and Marco Caccamo. Reset-based recovery for real-time cyber-physical systems with temporal safety constraints. In *2016 IEEE 21st International Conference on Emerging Technologies and Factory Automation (ETFA)*, pages 1–8. IEEE, 2016.
- [Abdi *et al.*, 2018] Fardin Abdi, Chien-Ying Chen, Monowar Hasan, Songran Liu, Sibin Mohan, and Marco Caccamo. Guaranteed physical security with restart-based design for cyber-physical systems. In *2018 ACM/IEEE 9th International Conference on Cyber-Physical Systems (ICCPS)*, pages 10–21. IEEE, 2018.
- [Berducci *et al.*, 2021] Luigi Berducci, Edgar A Aguilar, Dejan Ničković, and Radu Grosu. Hierarchical potential-based reward shaping from task specifications. *arXiv e-prints*, pages arXiv–2110, 2021.
- [Brockman *et al.*, 2016] Greg Brockman, Vicki Cheung, Ludwig Pettersson, Jonas Schneider, John Schulman, Jie Tang, and Wojciech Zaremba. Openai gym. *arXiv preprint arXiv:1606.01540*, 2016.
- [Burchfiel *et al.*, 2016] Benjamin Burchfiel, Carlo Tomasi, and Ronald Parr. Distance minimization for reward learning from scored trajectories. In *Proceedings of the AAAI Conference on Artificial Intelligence*, volume 30, 2016.
- [Chang *et al.*, 2019] Ya-Chien Chang, Nima Roohi, and Sicun Gao. Neural lyapunov control. *Advances in neural information processing systems*, 32, 2019.
- [Degris *et al.*, 2012] Thomas Degris, Patrick M Pilarski, and Richard S Sutton. Model-free reinforcement learning with continuous action in practice. In *2012 American Control Conference (ACC)*, pages 2177–2182. IEEE, 2012.
- [Deshmukh *et al.*, 2017] Jyotirmoy V Deshmukh, Alexandre Donzé, Shromona Ghosh, Xiaoqing Jin, Garvit Juniwal, and Sanjit A Seshia. Robust online monitoring of signal temporal logic. *Formal Methods in System Design*, 51(1):5–30, 2017.
- [Ding *et al.*, 2011] Xu Chu Ding, Stephen L Smith, Calin Belta, and Daniela Rus. Mdp optimal control under temporal logic constraints. In *2011 50th IEEE Conference on Decision and Control and European Control Conference*, pages 532–538. IEEE, 2011.
- [Donzé *et al.*, 2015] Alexandre Donzé, Vasumathi Raman, G Frehse, and M Althoff. Blustl: Controller synthesis from signal temporal logic specifications. *ARCH@ CPSWeek*, 34:160–8, 2015.
- [Fu and Topcu, 2014] Jie Fu and Ufuk Topcu. Probably approximately correct mdp learning and control with temporal logic constraints. *arXiv preprint arXiv:1404.7073*, 2014.
- [Haarnoja *et al.*, 2018] Tuomas Haarnoja, Aurick Zhou, Kristian Hartikainen, George Tucker, Sehoon Ha, Jie Tan, Vikash Kumar, Henry Zhu, Abhishek Gupta, Pieter Abbeel, et al. Soft actor-critic algorithms and applications. *arXiv preprint arXiv:1812.05905*, 2018.
- [Hamilton *et al.*, 2022] Nathaniel Hamilton, Preston K Robinetto, and Taylor T Johnson. Training agents to satisfy timed and untimed signal temporal logic specifications with reinforcement learning. In *International Conference on Software Engineering and Formal Methods*, pages 190–206. Springer, 2022.
- [Kong *et al.*, 2015] Jason Kong, Mark Pfeiffer, Georg Schildbach, and Francesco Borrelli. Kinematic and dynamic vehicle models for autonomous driving control design. In *2015 IEEE intelligent vehicles symposium (IV)*, pages 1094–1099. IEEE, 2015.
- [Kong *et al.*, 2018] Fanxin Kong, Meng Xu, James Weimer, Oleg Sokolsky, and Insup Lee. Cyber-physical system checkpointing and recovery. In *2018 ACM/IEEE 9th International Conference on Cyber-Physical Systems (ICCPS)*, pages 22–31. IEEE, 2018.
- [Li *et al.*, 2017] Xiao Li, Cristian-Ioan Vasile, and Calin Belta. Reinforcement learning with temporal logic rewards. In *2017 IEEE/RSJ International Conference on Intelligent Robots and Systems (IROS)*, pages 3834–3839. IEEE, 2017.
- [Li *et al.*, 2018] Xiao Li, Yao Ma, and Calin Belta. A policy search method for temporal logic specified reinforcement learning tasks. In *2018 Annual American Control Conference (ACC)*, pages 240–245. IEEE, 2018.
- [Ljung, 1998] Lennart Ljung. System identification. In *Signal analysis and prediction*, pages 163–173. Springer, 1998.
- [Lopez *et al.*, 2022] Diego Manzananas Lopez, Matthias Althoff, Luis Benet, Xin Chen, Jiameng Fan, Marcelo Forets, Chao Huang, Taylor T Johnson, Tobias Ladner, Wenchao Li, et al. Arch-comp22 category report: Artificial intelligence and neural network control systems (ainncs) for continuous and hybrid systems plants. In *Proceedings of 9th International Workshop on Applied*, volume 90, pages 142–184, 2022.
- [Ma *et al.*, 2021] Rui Ma, Sagnik Basumallik, Sara Eftekharijad, and Fanxin Kong. A data-driven model predictive control for alleviating thermal overloads in the presence of possible false data. *IEEE Transactions on Industry Applications*, 57(2):1872–1881, 2021.
- [Peters *et al.*, 2005] Jan Peters, Sethu Vijayakumar, and Stefan Schaal. Natural actor-critic. In *European Conference on Machine Learning*, pages 280–291. Springer, 2005.
- [Qin *et al.*, 2022] Zengyi Qin, Dawei Sun, and Chuchu Fan. Sablas: Learning safe control for black-box dynamical

- cal systems. *IEEE Robotics and Automation Letters*, 7(2):1928–1935, 2022.
- [Raffin *et al.*, 2021] Antonin Raffin, Ashley Hill, Adam Gleave, Anssi Kanervisto, Maximilian Ernestus, and Noah Dormann. Stable-baselines3: Reliable reinforcement learning implementations. *Journal of Machine Learning Research*, 22(268):1–8, 2021.
- [Raman *et al.*, 2014] Vasumathi Raman, Alexandre Donz e, Mehdi Maasoumy, Richard M Murray, Alberto Sangiovanni-Vincentelli, and Sanjit A Seshia. Model predictive control with signal temporal logic specifications. In *53rd IEEE Conference on Decision and Control*, pages 81–87. IEEE, 2014.
- [Sadraddini and Belta, 2018] Sadra Sadraddini and Calin Belta. Formal guarantees in data-driven model identification and control synthesis. In *Proceedings of the 21st International Conference on Hybrid Systems: Computation and Control (part of CPS Week)*, pages 147–156, 2018.
- [Silver *et al.*, 2014] David Silver, Guy Lever, Nicolas Heess, Thomas Degris, Daan Wierstra, and Martin Riedmiller. Deterministic policy gradient algorithms. In *International conference on machine learning*, pages 387–395. PMLR, 2014.
- [Todorov *et al.*, 2012] Emanuel Todorov, Tom Erez, and Yuval Tassa. Mujoco: A physics engine for model-based control. In *2012 IEEE/RSJ international conference on intelligent robots and systems*, pages 5026–5033. IEEE, 2012.
- [Trott *et al.*, 2019] Alexander Trott, Stephan Zheng, Caiming Xiong, and Richard Socher. Keeping your distance: Solving sparse reward tasks using self-balancing shaped rewards. *Advances in Neural Information Processing Systems*, 32, 2019.
- [Vardi, 1996] Moshe Y Vardi. An automata-theoretic approach to linear temporal logic. *Logics for concurrency*, pages 238–266, 1996.
- [Zhang *et al.*, 2020] Lin Zhang, Xin Chen, Fanxin Kong, and Alvaro A Cardenas. Real-time attack-recovery for cyber-physical systems using linear approximations. In *2020 IEEE Real-Time Systems Symposium (RTSS)*, pages 205–217. IEEE, 2020.
- [Zhang *et al.*, 2021] Lin Zhang, Pengyuan Lu, Fanxin Kong, Xin Chen, Oleg Sokolsky, and Insup Lee. Real-time attack-recovery for cyber-physical systems using linear-quadratic regulator. *ACM Transactions on Embedded Computing Systems (TECS)*, 20(5s):1–24, 2021.

Appendix A Detailed Experiment Setup

In this section, we show and explain the details of the experiments setup including benchmarks information and hyper-parameters of the framework.

A.1 Benchmarks

We have implemented our framework on four benchmarks as Table 5 shows. The four benchmarks have different numbers of dimensions of state space from 3 to 10, and numbers of dimensions of action space from 1 to 3. All of them are continuous systems as required by the training algorithms. All of them are non-linear systems except the DC Motor Position benchmarks.

The states of the DC Motor Position benchmark are the rotation angle, angular velocity and the current. The only control input for this benchmark is the voltage. The states of the Bicycle benchmark are the position coordinates, the orientation and the velocity. The control inputs of the bicycle benchmark are the steering angle and acceleration. The states for the Attitude Control benchmarks are the angular velocities from three dimensions and the rodrigues parameters. The control inputs for the attitude control benchmark are the torques. The states of the Swimmer benchmarks are the position coordinates, angle of the front tip, angle of the rotors, velocities of the tip, angular velocity of the tip and the angular velocities of the rotors. The control inputs are the torques of the two rotors.

The Swimmer benchmark is the most complex benchmark among the four benchmarks. The swimmer agent consists of at least three segments in a row, with every two consecutive segments connected by an articulation joint. The swimmer stays inside a two-dimensional pool and the objective is to move as quickly as possible to the right by applying torque to the rotors and utilizing fluid friction.

A.2 Hyper-parameters

	A2C	PPO
learning rate	7e-4	3e-4
update frequency	every 5 steps	every 2048 steps
gamma	0.99	0.99
value function coef	0.5	0.5
RMSProp epsilon	1e-5	NA
max gradient norm	0.5	0.5

Table 3: Hyper-parameters of A2C and PPO

	DDPG	TD3	SAC
learning rate	1e-3	3e-4	3e-4
batch size	100	100	256
buffer size	1e6	1e6	1e6
gamma	0.99	0.99	0.99
soft update coefficient	5e-3	5e-3	5e-3

Table 4: Hyper-parameters of DDPG,TD3 and SAC

There are several hyper-parameters in our algorithm including training and testing. For all trials, we have the following two hyper-parameters.

(1) Maximum trace length during training. This hyper-parameter is set to 30 for all benchmarks except swimmer which is set to 50, and it remains the same as the maximum deadline in the testing phase. It is significant to choose an appropriate maximum trace length for training. On one hand, if it is too short, the system may not have enough time to reach the target set based on physical laws. If the system can never touch the target set during training, our framework will degenerate and cannot get encouragement from ASAP. On the other hand, if the maximum trace length is too long, it takes more steps for training and becomes time-consuming. Assuming the number of training steps is fixed, the longer maximum trace length is, the fewer number of traces will be explored. Insufficient exploration can be a reason for performance decay, since each trace starts from a random initial point in state space, and less proportion of the state space is explored since less number of traces are experienced. If this parameter is set to larger values such as 40 or 60, the agents can achieve a similar trend with more training steps.

(2) Total number of training steps. This hyper-parameter is set to 1e6 for DC Motor Position benchmarks, 3e6 for bicycle benchmark and Attitude Control benchmark, and 6e6 for Swimmer benchmarks. Intuitively, the more complex the system dynamics are, the more training steps are required for convergence. More evidence can be found in Appendix B.

We then list some important hyper-parameters specific to the training algorithms of our implementation in Table 3 and 4. Specifically, Table 3 shows the hyper-parameters for A2C and PPO algorithm, explained as follows.

1. The value function coef stands for the value function coefficient for the loss calculation.
2. RMSProp is a variation of the AdaGrad method and achieves good performance on various problems especially non-convex optimization. The RMSProp Epsilon stabilizes square root computation in RMSProp update denominator.
3. The maximum gradient norm control the gradient clip range.

Aside from the above, the PPO algorithm has a factor 0.95 for trade-off between bias and variance for generalized advantage estimator. And for every 10 epochs, the surrogate loss will be optimized again.

Moreover, Table 4 shows the details of DDPG, TD3 and SAC algorithms of our experiments, explained as follows.

1. The learning rate of DDPG is greater than other algorithms. This setting is general for training.
2. The buffer size is greater than the training steps for our experiments. In other words, we don't pop out samples from the replay buffer during the training.

Aside from above, the networks for all algorithms are multi-layer perceptrons.

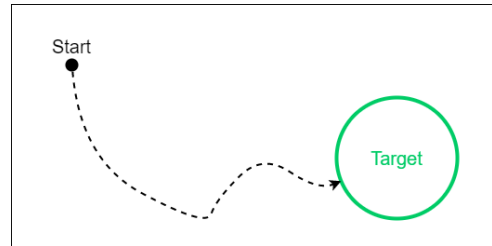
A.3 Tasks details

We consider two kinds of tasks in our experiments: *Reach* task and *Reach&Avoid* task as Fig. 3 shows. We do not make any assumption of the initial state.

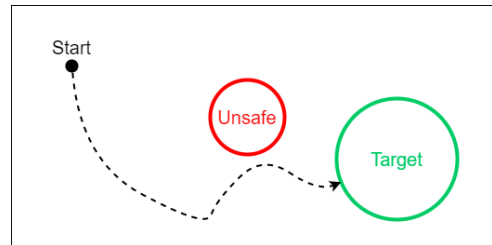
	DC Motor Position	Bicycle
# state dims	3	4
# action dims	1	2
linearity	linear	non-linear
continuity	continuous	continuous
target center	$[\pi/2, 0, 0]$	$[1, 1, 0, \sqrt{2}]$
target radius	0.5	0.8
unsafe center	$[\pi/4, 0, 0]$	$[0.5, 0.5, 0, \sqrt{2}/2]$
unsafe radius	0.2	0.3

	Attitude Control	Swimmer
# state dims	6	10
# action dims	3	2
linearity	non-linear	non-linear
continuity	continuous	continuous
target center	$[0, 0, 0, 0, 0, 0]$	$[0, 9, 0, 0, 0, 0, 0, 0, 0, 0]$
target radius	0.8	0.8
unsafe center	$[0, 0, 0.2, 0, 0, 0]$	$[0, 0.6, 0, 0, 0, 0, 0, 0, 0, 0]$
unsafe radius	0.3	0.3

Table 5: Benchmark Details



(a) *Reach* task



(b) *Reach&Avoid* task

Figure 3: Task examples

The STL specification format for Reach&Avoid tasks as follow:

$$F_{[0,10]}(\text{Euclid}(\text{target}) \leq r_t \text{ and } G_{[0,\infty]}(\text{Euclid}(\text{unsafe}) > r_u) \quad (16)$$

The former part of the formula is φ_T for reach task and latter part is φ_O for avoid task as defined in section 4.3. We want to achieve φ_T ASAP. *Euclid* is the euclidean distance on the

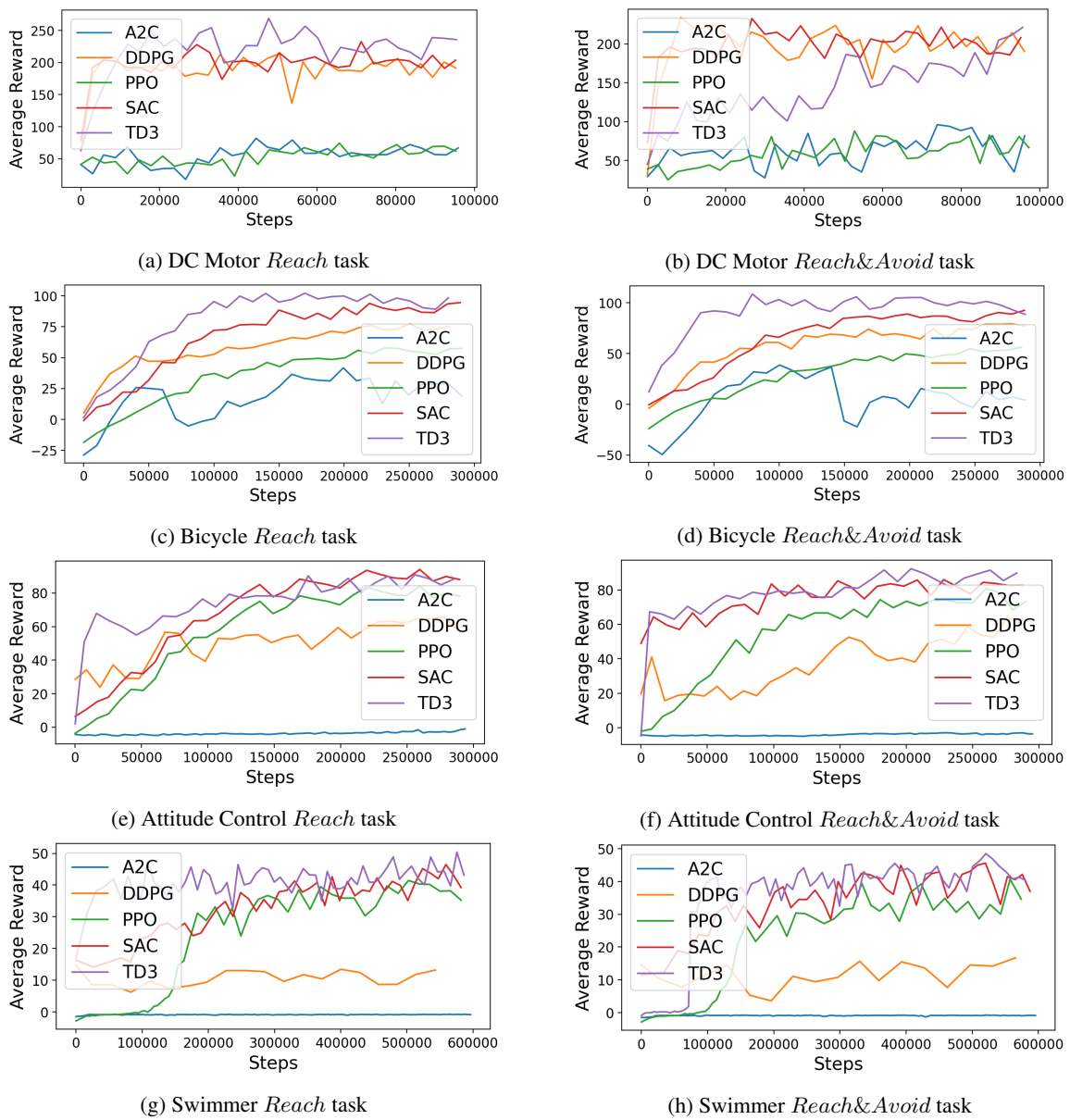


Figure 4: Progression of average reward during training on different tasks.

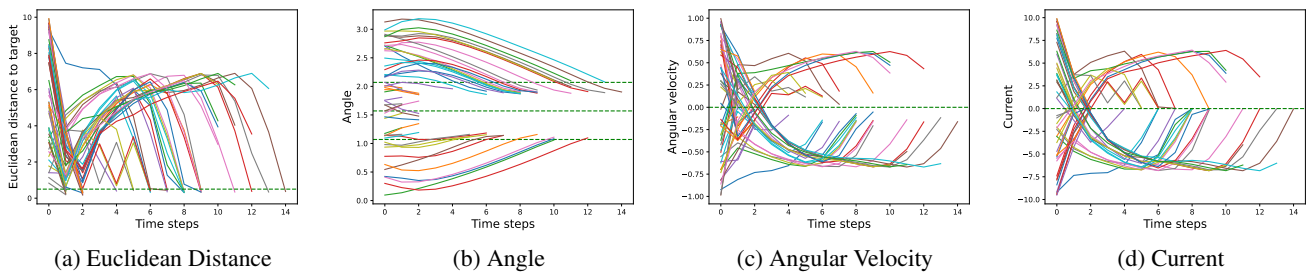


Figure 5: Example testing trajectories of *Reach* Task on DC Motor Position Benchmark

state space, r_t is the radius of the target set, r_u is the radius of the unsafe set which are specifies in Table 5.

Appendix B Detailed Experiment Results

In this section, we show more detailed experiment results for ablation studies.

B.1 Ablation Study 1

The series figures showed the training history of different algorithms for different tasks on different benchmarks.

On DC Motor Position benchmark, the training takes 1e6 steps and TD3, SAC and DDPG have similar performance and outperform PPO and A2C.

On Attitude Control benchmark and Bicycle benchmark, the training takes 3e6 steps. The average reward is still increasing after 1e6 as Fig. 4 shows. This echos the intuition we have in appendix A.

On swimmer benchmark, the the training takes 6e6 steps. SAC and TD3 outperform other algorithms.

B.2 Ablation Study 2

In this subsection, we discuss alternative ways to achieve ASAP and their performance. Intuitively, greedy algorithm can solve this problem. We can force the system to move closer and closer to the target set on each step. However, this method is not guaranteed to work since the system dynamics follow the physical law.

Fig. 5 shows an example of the change of euclidean distance to the target and system states for a reach task. The goal is to reach $[\pi/2, 0, 0, 0]$ ASAP. There are 50 trajectories on each figure, the euclidean distance is not monopoly decreasing since the transition of current and angular velocity are required to drive the angle to target, which is determined by the system dynamics. Respectively, the success rate of greedy algorithm for the *Reach* task on the DC Motor Position benchmark is 67.6%. Additionally, it is hard to design how much each step the system is closer to the target set compare to the previous step(step movement constant) since the system dynamics is not known.

Another way to express ASAP is transform the greedy algorithm as a STL-specification which turns to encourage the system to move closer and closer to the target. However, STL does not have the capability to express ASAP and the the success rate of greedy algorithm for the *Reach* task on the DC Motor Position benchmark is 55.3%.

For the STL-specification of reach, we use finally operator (F) and corresponding semantics. In natural language, the meaning of this specification is "finally reach the target set". It is also possible to change it to the globally operator (G) and the trained agents have similar performance.

To be noticed, quantitative semantics of STL is not our contribution. And we have tested if the we use the above alternative ways and ASAP-Phi together on the same task, it can achiever success rate over 95%. This result partially shows the necessity of our framework.

Appendix C Explanation of the Main Proof

In this appendix section, we further explain the proof of Theorem 2 in Section 4.2 with illustrations.

Overall, the proof aims to show that optimality of a policy of ASAP-Phi implies that it is an ASAP policy. Equivalently, we can show that the existence of an optimal and non-ASAP policy implies a contradiction. Therefore, we assume for the existence of such a policy π^* , which favors a trajectory \bar{s}^* that satisfies the property later than an alternative trajectory \bar{s}' due to its non-ASAP nature. These two trajectories are illustrated back in Section 4.2, and we re-draw it here again for convenience as Figure 6.

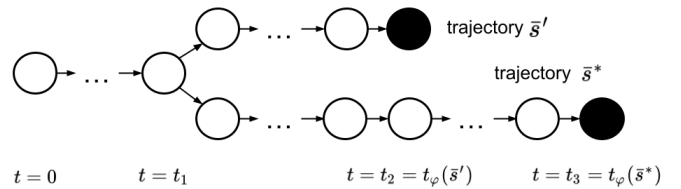


Figure 6: The two existing trajectories under the assumed π^* . An empty circle represents the trajectory so far does not satisfy φ , while a filled circle means satisfy.

Next, because of Assumption 1, it is feasible to maintain \bar{s}' satisfactory until time step t_3 . That is, a trajectory \bar{s}'' that extends \bar{s}' until t_3 , and it keeps property satisfaction all the way from t_2 to t_3 . This is illustrated in Figure 7.

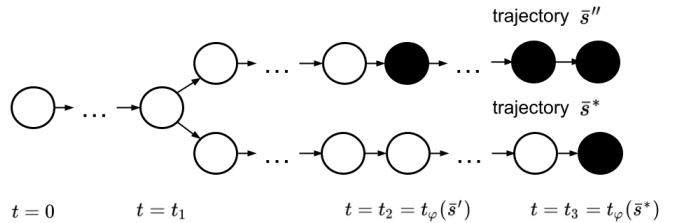


Figure 7: Trajectory \bar{s}'' extends from \bar{s}' and keeps property satisfaction from t_2 to t_3 .

To show that the current policy π^* that favors \bar{s}^* more than \bar{s}' (and therefore more than \bar{s}''), we need to show that it does not maximize the state value function on all states. Specifically, we pick the common initial state s_0 of both the traces, and compute the value at this state under policy π^* . Overall, the value can be split into four portions, as illustrated in Figure 8.

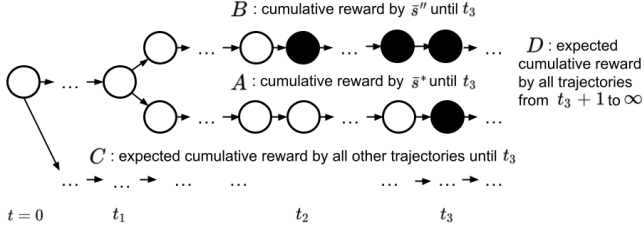


Figure 8: Value at s_0 is split into four parts: $p_{\bar{s}^*} A$, $p_{\bar{s}''} B$, C and D .

The split is deduced by Equations (8) and (9) in the proof. Overall, denote the probability (under some policy) of taking trajectory \bar{s}^* and \bar{s}'' as $p_{\bar{s}^*}$ and $p_{\bar{s}''}$, respectively. Regardless of the policy, the four portions are

1. The expected cumulative reward from taking trajectory \bar{s}^* from beginning to t_3 , i.e., $p_{\bar{s}^*} A$,
2. The expected cumulative reward from taking trajectory \bar{s}'' from beginning to t_3 , i.e., $p_{\bar{s}''} B$,
3. The expected cumulative reward from taking any other trajectory aside from these two, from beginning to t_3 , i.e., C , and
4. The expected cumulative reward from taking any trajectory from $t_3 + 1$ to ∞ , i.e., D .

Therefore, for any policy π , we have the value at state s_0 as

$$v_{\pi}^*(s_0) = p_{\bar{s}^*} A + p_{\bar{s}''} B + C_{\pi} + D_{\pi}. \quad (17)$$

Notice that A and B are deterministic terms and are independent of any policy distribution, but C and D are expected values, so they are parameterized by the distribution π .

Under our assumed optimal policy π^* , the policy favors \bar{s}^* more than \bar{s}'' , i.e., $p_1 = p_{\bar{s}^*} > p_{\bar{s}''} = p_2$ under π^* , we have

$$v_{\pi^*}^*(s_0) = p_1 A + p_2 B + C_{\pi^*} + D_{\pi^*}. \quad (18)$$

After finding this split of value, we seek an alternative policy π' , which has a higher value $v_{\pi'}^*(s_0) > v_{\pi^*}^*(s_0)$, and therefore π^* does not maximize the value at state s_0 and is not optimal, so that a contradiction occurs.

As stated in the main proof, we construct the alternative policy π' by swapping the probabilities of taking trajectories \bar{s}'' and \bar{s}^* , while the probabilities on everything else remain the same. This give us $p_{\bar{s}''} = p_1$ and $p_{\bar{s}^*} = p_2$, i.e.,

$$v_{\pi'}^*(s_0) = p_2 A + p_1 B + C_{\pi'} + D_{\pi'}. \quad (19)$$

From Equation (10) to the end of the proof, we compare the two values term-by-term. This procedure indeed shows that $v_{\pi'}^*(s_0) > v_{\pi^*}^*(s_0)$ and reaches the contradiction.